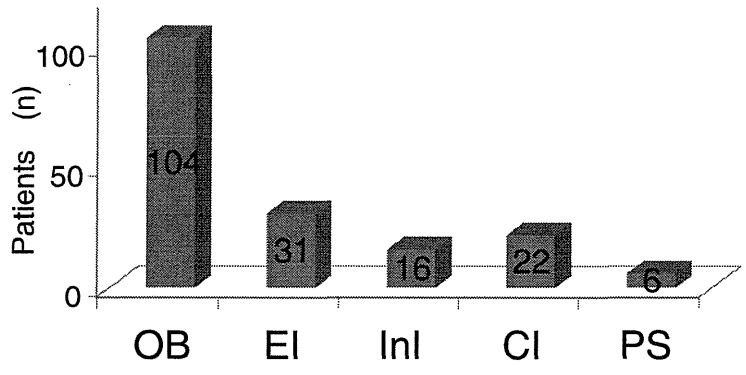

Figure 2 Incidence of clinically metastatic pelvic lymph nodes in each region. *Including duplication.

regions or sub-regions. We defined each of these regions as a NSR (non-solitary region). Patients with NSR metastases had high FIGO stages or a large number of positive nodes. Patients with high FIGO-stage disease (III, IVA) had a significantly higher frequency of positive nodes in the NSR (23/54, 43%) compared with patients who had low FIGO-stage disease (15/60, 25%) (P=0.047). The average number of metastatic lymph nodes was 3.7 for patients with NSR and 1.9 for patients with non-NSR. There was no significant relationship between tumor diameter and the incidence of NSR metastases: 6/18 (30%) for tumors≤40 mm, 20/58 (34%) for tumors 41–60 mm, and 15/38 (38%) for tumors≥61 mm. All 16 patients with nodal metastases in less common (≤ 6/114, 5%) areas (presacral, caudal obturator, and caudal/lateral external iliac regions) had large tumors (> 4 cm), of which all 9 cases who had NSR metastases in the lateral external iliac and presacral regions were stage IIB or more. In addition, all 9 cases with NSR metastases in the caudal obturator or caudal external iliac regions also had positive lymph nodes in the ipsilateral cranial obturator or medial external iliac region, and all 3 cases with NSR metastases in the lateral external iliac region had positive nodes in the ipsilateral intermediate external iliac region.

Discussion

To minimize the risk of inter-planner variability on pelvic node CTV contouring, consensus-based CTV guidelines have been developed for patients with cervical cancer [2-4]. Modification of the standard CTV guidelines based on the probability of subclinical disease, in other words, risk of recurrence is the next challenge for individualized treatment planning.

The CTV could be divided into subgroups, e.g., high-risk CTV and low-risk CTV, according to the probability of recurrence. The high-risk CTV would be defined as the volume that involves frequent metastases, and should be treated for every patient. In contrast, the low-risk CTV would be defined as a region with rare disease involvement, and might be able to be excluded from the CTV in certain situations. The arrangement of CTV nodes could reduce the dose/volume of organs at risk (OAR) and lead to lower side effects. In the previously published guidelines, the CTV nodes cover the entire anatomical pelvic node distribution [2-4,6]. The guidelines did not emphasize the actual probability of nodal involvement, in other words, the risk of recurrence. In head and neck cancers, individualization of CTV nodes for 3D planning was proposed according to the primary

Table 2 Number of patients* with clinically pelvic nodal metastases # by region/subdivided region

	Total	OB		EI				InI	CI	PS
		Cranial	Caudal	Med	Int	Lat	Caudal			
Positive nodes in other regions	82	76	5	10	13	3	6	16	22	6
No positive nodes in other regions	32	28	0	2	2	0	0	0	0	0
Total	114	104	5	12	15	3	6	16	22	6

*including duplication, # assesed by CT/MRI (>= 10 mm in shortest diameter).
OB = obturator region, EI = external iliac region, InI = internal iliac region, CI = common iliac region, PS = presacral region, Med = medial, Int = intermediate, Lat = lateral.

site or T/N stage [8]. For uterine cervical cancer, in an attempt at dose reduction for OAR, small pelvic field irradiation has been investigated [9,10]. The treatment fields were designed to exclude the common iliac region. In this study, we tried to analyze the 3D distribution patterns of positive nodes in the pelvis assessed by pretreatment CT/MRI to quantify the nodal metastasis probability in patients with uterine cervical cancer.

Some surgical series have indicated that the obturator and external iliac regions have the highest frequency of metastatic lymph nodes [11,12]. This is consistent with the findings demonstrated in the present study. We subdivided the obturator and external iliac regions according to craniocaudal distribution at the border of the femoral head. Analyses with this subdivision revealed that positive lymph nodes were rarely seen on the caudal side, and most were observed on the cranial side. Benedetti and colleagues also subdivided the obturator region into deep and superficial regions. They demonstrated that there were few metastatic lymph nodes in the deep region [12]. Our results are consistent with that report. No previous study supports our finding that the caudal external iliac sub-region rarely had positive nodes. However, the present results suggest the appropriateness of the definition of the external iliac region in the RTOG and JCOG guidelines, which set the lower end of the external iliac region at the top of the femoral head [2,4].

For the external iliac region above the aspect of the femoral head, 3 anatomically subdivided regions have been proposed [6,7]. According to the definition, positive nodes in the medial external iliac and intermediate external iliac regions were frequent in contrast to the lateral external iliac regions in our study. This observation was also made by Graham et al. [13]. Taylor et al. demonstrated that the normal node distribution extended more than 10 mm laterally to the external iliac artery and veins in their USPIO MRI study. Based on this finding, they recommended that the CTV should expand 17 mm laterally from the vessels to cover the region sufficiently [6]. However, our present study demonstrated that positive nodes were rare in the lateral external iliac region, and suggested that the expansion that Taylor proposed could be omitted in some cases.

Based on the findings from our present analyses, high-risk regions such as the cranial obturator and the medial and intermediate external regions must be irradiated sufficiently in all cases. In contrast, the caudal external iliac, caudal obturator, lateral external iliac and presacral regions, which demonstrated a very low incidence (≤ 5%) of positive nodes, might be allowed to be excluded in patients who satisfy all of the following criteria: small tumor size (≤ 4 cm) and no positive nodes on CT/MRI. The CTV shrinkage might help to reduce complications in the surrounding organs. Further investigation is needed to justify such modification in clinical practice. In the other remaining regions (i.e., common iliac, internal iliac), although no patient in this study had a solitary positive lymph node, the positive rate was not low. Therefore, we suggest that the common iliac and internal iliac regions should continue to be included in all cases for radical radiotherapy for patients with uterine cervical cancer.

This study has some limitations. First, the insufficient sensitivity of CT/MRI is critical. Bellomi and colleagues reported that the sensitivity and specificity of CT were 64% and 93%, respectively, and those of MRI were 72% and 93%, respectively [14]. The results of this study should be interpreted carefully due to the inadequate sensitivity and specificity of these methods. Meanwhile, Choi and coworkers compared the sensitivity and specificity of MRI and positron emission tomography/computed tomography (PET/CT) [15]. With MRI, the sensitivity and specificity were 30% and 92%, respectively, and with PET/CT, the sensitivity and specificity were 57% and 92%, respectively. Further study using PET/CT is encouraged. Second, the absence of histopathological confirmation is a serious weakness of the present study. Although some surgical series presented detailed data on the pathological positive node distribution [11,12], data for inoperable advanced-stage patients were sparse. In addition, it is difficult to apply the distribution of metastatic nodes from surgical findings directly to the 3D distribution on CT/MRI images for accurate CTV contouring. For these reasons, despite its insufficient sensitivity and specificity, some surrogate information could be obtained from the study using CT/MRI. Third, this study consists of a relatively small number of patients and a heterogenous population (i.e. stage, tumor size). Various systematic and random errors due to multicenter assessment over a long time period might negatively affect the validity of the study.

Conclusions

The present study demonstrated distribution patterns of positive pelvic nodes in patients with cervical cancer treated with definitive radiotherapy/chemoradiotherapy. The findings might contribute to future investigations for the individualization of CTV node contouring.

Abbreviations

3D: Three-dimensional; CT: Computed tomography; MRI: Magnetic resonance imaging; FIGO: Federation Internationale de Gynecologie et de Obstetrique; RTOG: Radiation Therapy Oncology Group; UK: United Kingdom; JCOG: Japan Clinical Oncology Group; CTV: Clinical target volume; NSR: Non-solitary region; OAR: Organs at risk; PET: Positron emission tomography.

Competing interests

The authors declare that they have no competing interests regarding this manuscript.

Authors' contributions
GK and TT designed this study, assembled the data, performed the statistical analysis and interpretation, and wrote the manuscript. KF, TK, TO, YK, RY, and TU provided study materials from each institution and proofed the manuscript. AY participated as a diagnostic radiologist and confirmed the distribution of positive lymph nodes. SI and MH helped to revise the manuscript. All authors read and approved the final manuscript.

Acknowledgment
This study was supported in part by the Grant-in-Aid for Cancer Research (20S-5) from the Ministry of Health, Labor and Welfare, Japan and National Center Research and Development Fund (23-A-21).

Author details
[1]Department of Radiology, Graduate School of Medical Science, University of the Ryukyus, Okinawa, Japan. [2]Department of Radiation Oncology, Aichi Cancer Center, Nagoya, Japan. [3]Heavy Ion Medical Center, Gunma University, Maebashi, Japan. [4]Department of Radiation Oncology, Graduate School of Biomedical Sciences, Hiroshima University, Hiroshima, Japan. [5]Department of Radiology, Tokyo Medical and Dental University, Tokyo, Japan. [6]Department of Radiology, Graduate School of Medicine, Chiba University, Chiba, Japan. [7]Department of Radiation Oncology, Juntendo University, Tokyo, Japan. [8]Department of Radiation Oncology and Image-applied Therapy, Kyoto University Graduate School of Medicine, Kyoto, Japan.

Received: 22 January 2013 Accepted: 1 June 2013
Published: 8 June 2013

References

1. Roeske JC, Lujan A, Mundt AJ, *et al*: **Intensity-modulated whole pelvic radiation therapy in patients with gynecologic malignancies.** *Int J Radiat Oncol Biol Phys* 2000, **48**:1613–1621.
2. Small W Jr, Mell LK, Anderson P, *et al*: **Consensus guidelines for delineation of clinical target volume for intensity-modulated pelvic radiotherapy in postoperative treatment of endometrial and cervical cancer.** *Int J Radiat Oncol Biol Phys* 2008, **71**:428–434.
3. Vilarino-Varela MJ, Taylor A, Rockall AG, *et al*: **A verification study of proposed pelvic lymph node localisation guidelines using nanoparticle-enhanced magnetic resonance imaging.** *Radiother Oncol* 2008, **89**:192–196.
4. Toita T, Ohno T, Kaneyasu Y, *et al*: **A consensus-base guideline defining the clinical target volume for pelvic lymph nodes in external beam radiotherapy for uterine cervical cancer.** *Jpn J Clin Oncol* 2010, **40**:456–463.
5. World Medical Association Declaration of Helsinki: **Ethical principles for medical research involving human subjects.** *JAMA* 2000, **284**:3043–3045.
6. Taylor A, Rockall AG, Reznek RH, *et al*: **Mapping pelvic lymph nodes: guidelines for delineation in intensity-modulated radiotherapy.** *Int J Radiat Oncol Biol Phys* 2005, **63**:1604–1612.
7. Lengelé B, Scalliet P: **Anatomical bases for the radiological delineation of lymph node areas. Part III: Pelvis and lower limbs.** *Radiother Oncol* 2009, **92**:22–33.
8. Grégoire V, Eisbruch A, Hamoir M, *et al*: **Proposal for the delineation of the nodal CTV in the node-positive and the post-operative neck.** *Radiother Oncol* 2006, **79**:15–20.
9. Ohara K, Tsunoda H, Satoh T, *et al*: **Use of the small pelvic field instead of the classic whole pelvic field in postoperative radiotherapy for cervical cancer: reduction of adverse events.** *Int J Radiat Oncol Biol Phys* 2004, **60**:258–264.
10. Oike T, Ohno T, Wakatsuki M, *et al*: **The benefit of small bowel and pelvic bone sparing in excluding common iliac lymph node region from conventional radiation fields in patients with uterine cervical cancer: a dosimetric study.** *J Radiat Res* 2010, **51**:715–721.
11. Sakuragi N, Satoh C, Takeda N, *et al*: **Incidence and distribution pattern of pelvic and paraaortic lymph node metastasis in patients with Stages IB, IIA, and IIB cervical carcinoma treated with radical hysterectomy.** *Cancer* 1999, **85**:1547–1554.
12. Benedetti-Panici P, Maneschi F, Scambia G, *et al*: **Lymphatic spread of cervical cancer: an anatomical and pathological study based on 225 radical hysterectomies with systematic pelvic and aortic lymphadenectomy.** *Gynecol Oncol* 1996, **62**:19–24.
13. Perez CA: *Uterine Cervix: principles and Practice of Radiation Oncology.* 3rd edition. Philadelphia: Lippincott-Raven; 1998:1736.
14. Bellomi M, Bonomo G, Landoni F, *et al*: **Accuracy of computed tomography and magnetic resonance imaging in the detection of lymph node involvement in cervix carcinoma.** *Eur Radiol* 2005, **15**:2469–2474.
15. Choi HJ, Roh JW, Seo SS, *et al*: **Comparison of the accuracy of magnetic resonance imaging and positron emission tomography/computed tomography in the presurgical detection of lymph node metastases in patients with uterine cervical carcinoma: a prospective study.** *Cancer* 2006, **106**:914–922.

doi:10.1186/1748-717X-8-139
Cite this article as: Kasuya *et al.*: Distribution patterns of metastatic pelvic lymph nodes assessed by CT/MRI in patients with uterine cervical cancer. *Radiation Oncology* 2013 8:139.

Hepatology Research

Hepatology Research 2013; 43: 717–727 doi: 10.1111/hepr.12007

Original Article

Dynamic computed tomography appearance of tumor response after stereotactic body radiation therapy for hepatocellular carcinoma: How should we evaluate treatment effects?

Tomoki Kimura,[1] Shigeo Takahashi,[1] Masahiro Kenjo,[1] Ikuno Nishibuchi,[1] Ippei Takahashi,[1] Yuki Takeuchi,[1] Yoshiko Doi,[1] Yuko Kaneyasu,[1] Yuji Murakami,[1] Yoji Honda,[2] Hiroshi Aikata,[2] Kazuaki Chayama[2] and Yasushi Nagata[1]

[1]*Department of Radiation Oncology, Graduate School of Biomedical Sciences, Hiroshima University, Hiroshima, Japan and* [2]*Department of Medicine and Molecular Science, Division of Frontier Medical Science, Programs for Biomedical Research, Graduate School of Biomedical Sciences, Hiroshima University, Hiroshima, Japan*

Aim: To evaluate the dynamic computed tomography (CT) appearance of tumor response after stereotactic body radiation therapy (SBRT) for hepatocellular carcinoma (HCC) and reconsider response evaluation criteria for SBRT that determine treatment outcomes.

Methods: Fifty-nine patients with 67 tumors were included in the study. Of these, 56 patients with 63 tumors underwent transarterial chemoembolization using lipiodol prior to SBRT that was performed using a 3-D conformal method (median, 48 Gy/four fractions). Dynamic CT scans were performed in four phases, and tumor response was evaluated by comparing tumor appearance on CT prior SBRT and at least 6 months after SBRT. The median follow-up time was 12 months.

Results: The dynamic CT appearance of tumor response was classified into the following: type 1, continuous lipiodol accumulation without early arterial enhancement (26 lesions, 38.8%); type 2, residual early arterial enhancement within 3 months after SBRT (17 lesions, 25.3%); type 3, residual early arterial enhancement more than 3 months after SBRT (19 lesions, 28.4%); and type 4, shrinking low-density area without early arterial enhancement (five lesions, 7.5%). Only two tumors with residual early arterial enhancement did not demonstrate remission more than 6 months after SBRT.

Conclusion: The dynamic CT appearance after SBRT for HCC was classified into four types. Residual early arterial enhancement disappeared within 6 months in most type 3 cases; therefore, early assessment within 3 months may result in a misleading response evaluation.

Key words: dynamic computed tomography appearance, hepatocellular carcinoma, stereotactic body radiation therapy

INTRODUCTION

HEPATOCELLULAR CARCINOMA (HCC) is closely associated with hepatitis B virus (HBV) or hepatitis C virus (HCV) infections and the increasing prevalence of viral infections has led to an increased incidence of HCC. The curative therapy for HCC involves surgery including resection or transplantation.[1,2] However, only 10–30% patients initially presenting with HCC would be eligible for surgery either due to liver dysfunction, underlying cirrhosis or presence of multifocal tumors arising from viral infection.[3] For such patients, locoregional therapies such as ablative therapies or transarterial chemoembolization (TACE) are recommended.[1,2] Radiation therapy is a locoregional therapy that can be considered as an alternative to ablation/TACE or when these therapies have failed.[1] Recently, advances in imaging and radiation techniques that deliver high doses of radiation to focal HCC have helped to avoid

Correspondence: Dr Tomoki Kimura, Department of Radiation Oncology, Graduate School of Biomedical Sciences, Hiroshima University, 1-2-3 Kasumi, Minami-ku, Hiroshima City 734-8551, Japan. Email: tkkimura@hiroshima-u.ac.jp

This work was partly presented at the 53rd Annual Meeting of American Society for Therapeutic Radiology and Oncology (ASTRO), Miami, FL, USA, October 1–5 2011.

Conflict of interest: none.

Received 1 July 2012; revision 30 September 2012; accepted 15 October 2012.

radiation-induced liver damage (RILD). Several studies have reported good treatment outcomes with either stereotactic body radiation therapy (SBRT) or particle therapy with or without TACE for HCC,[4–7] and experience with radiation therapy for HCC has increased rapidly during the past decade.[8] These reports used various methods, such as the Response Evaluation Criteria in Solid Tumors (RECIST),[9] the World Health Organization (WHO) response evaluation criteria,[10] and dynamic CT with or without tumor enhancement[5] to evaluate tumor response. However, no significant progress has been made in establishing a consensus from the various studies that have evaluated the response of HCC to SBRT or particle therapy. Furthermore, no detailed studies have reported the use of CT to monitor tumor response after SBRT or particle therapy. It is extremely important to record the CT appearance at regular intervals to accurately evaluate tumor response because HCC demonstrates changes with time after SBRT.

The purpose of our study was to evaluate the dynamic CT appearance of tumor response after SBRT in conjunction with TACE for HCC and to reconsider response evaluation criteria for SBRT to determine treatment outcomes.

METHODS

Patient background

FROM MARCH 2002 to December 2011, 73 patients with 88 tumors underwent SBRT at our institution. Our study included 59 patients with 67 tumors who were analyzed using dynamic CT for more than 6 months after SBRT. There were 37 men and 22 women with a median age of 71 years (range, 49–90), including five patients with chronic hepatitis B and 47 patients with chronic hepatitis C. Six patients simultaneously underwent SBRT for two tumors each and two patients each with a solitary tumor were treated at different times. The inclusion criteria for curative SBRT were as follows: (i) patients over 20 years of age; (ii) an Eastern Cooperative Oncology Group Performance Status (ECOG PS) of 0–2; (iii) Child–Pugh score A or B; (iv) less than three HCC nodules, each up to 50 mm in diameter, without portal venous thrombosis or extrahepatic metastases; (v) inoperable patients because of their poor general condition or refusal of surgery; and (vi) patients unsuitable for radiofrequency ablation (RFA) because of tumor location (e.g. on the liver surface and near the porta hepatis), invisibility of tumor on ultrasonography or bleeding tendency. The exclusion criterion was presence of uncontrolled ascites. The majority of patients had previously undergone surgery or ablation therapies, and SBRT was recommended when these options were limited by technical difficulties or if the patient was inoperable or refused surgery. The clinical characteristics of the patients including age, sex, type of viral infection, Child–Pugh score, primary tumor location and size, ECOG PS and previous treatments are summarized in Table 1.

Hepatocellular carcinoma was diagnosed by its characteristic appearance of early enhancement in the arterial phase and hypodensity in the portal venous phase, which was revealed in most of the patients using either dynamic CT or angiography combined with CT. However, for five patients in whom these CT appearance were not observed, HCC was diagnosed histologically.

Treatment procedure

Before SBRT, 56 patients with 63 HCC underwent TACE using iodized lipiodol (lipiodol). Anticancer chemotherapies, such as epirubicin, cisplatin combined with lipiodol (7–70 mg/body at a concentration of 10 mg/mL lipiodol) or miriplatin mixed with lipiodol (20–80 mg/body at a concentration of 20 mg/mL lipiodol), administrated by injecting the drug into the hepatic artery feeding a segment or subsegments of the target tumor. The selected dose was based on tumor size and liver function. A small amount of gelatin sponge particles was used to induce embolization until the flow through the feeding artery was markedly decreased. The median time interval between TACE and SBRT was 1 month (range, 1–7). The interval was 1–2 months in most of the patients, but was 6–7 months in four patients. They were treated only with TACE because two patients were elderly and had some complications, and the other two patients wanted to be treated only with TACE at first.

Stereotactic body radiation therapy was performed using a 3-D conformal method in which a single high dose is delivered to the tumor. A vacuum cushion (Vac-Lok; CIVCO, Kalona, IA, USA) was used to immobilize the patient. Respiratory motion was evaluated using an X-ray simulator. If respiratory motion was greater than 5 mm, it was coordinated by either voluntary breath-holding using a spirometer or Abches (APEX Medical, Tokyo, Japan), which is a device that allows the patient to control the respiratory motion of their chest and abdomen. Patients held their breath in the end-expiratory phase because the interbreath-hold reproducibility of organ position in end-expiratory phase was better than that in the end-inspiratory phase.[11] This

Table 1 Patients background

Age	49–90 (median, 71)	Tumor size	3–54 mm (median, 19 mm)
Sex		Tumor location	
Male	37 patients	S1	1 lesion
Female	22 patients	S2	1 lesion
ECOG PS		S3	4 lesions
0	55 patients	S4	12 lesions
1	3 patients	S5	8 lesions
2	1 patient	S6	6 lesions
Type of viral infection		S7	15 lesions
HBV	5 patients	S8	20 lesions
HCV	47 patients	Previous treatment	
NBNC	7 patients	Surgery	21 patients
Child–Pugh class		RFA	17 patients
A	46 patients	PEI	9 patients
B	13 patients	TACE	56 patients
Child–Pugh score			
5	33 patients		
6	13 patients		
7	8 patients		
8≧	5 patients		

ECOG PS, Eastern Cooperative Oncology Group Performance Status; HBV, hepatitis B virus; HCV, hepatitis C virus; NBNC, non-hepatitis B non-hepatitis C; PEI, percutaneous ethanol injection; RFA, radiofrequency ablation; TACE, transcatheter arterial chemoembolization.

method was employed in 55 patients with 62 tumors. The free-breathing method was used in two patients with three tumors, and respiratory-gating using the Real-time Position Management (RPM) system (Varian Medical Systems, Palo Alto, CA, USA) was used in two patients with two tumors. For simulation, dynamic CT scans (Lightspeed QX/I; GE Medical Systems, Waukesha, WI, USA), including non-enhanced and contrast-enhanced scans, were performed in four phases, before contrast enhancement, and arterial, portal and venous phases. CT was performed using bolus injection of non-ionic iodinated contrast material (100 mL at a rate of 3 mL/s). CT volume data in the arterial phase were transferred to a 3-D treatment planning system (Pinnacle^3 ver. 9.0; Phillips Medical Systems, Fitchburg, WI, USA). Gross tumor volume (GTV) was defined as the volume of tumor containing the remains of lipiodol used with TACE and from early enhancement in the arterial phase of dynamic CT. A clinical target volume (CTV) margin of 3 mm was usually added to GTV for subclinical invasion. A planning target volume (PTV) margin of 5–8 mm, which included the reproducibility of respiratory motion and setup error to CTV, was usually added. Eight non-coplanar ports were selected in all patients, including four or five coplanar beams and three or four non-coplanar beams in a direction that avoided the stomach, intestine, gall bladder and spine, if possible. The prescribed dose and fractionations were 60 Gy/eight fractions in 10 tumors, 50 Gy/five fractions in five tumors, 40 Gy/four fractions in one tumor and 48 Gy/four fractions in 51 tumors. Beams were delivered using 6–10-MV photons of linear accelerator (CLINAC 2300 C/D or iX; Varian Medical Systems, Palo Alto, CA, USA) that delivered 600 monitor units/min so that the duration of breath-holding could be 15 s or less for each treatment field.

Evaluation

Follow-up dynamic CT was performed every 1–3 months after SBRT. Serum HCC-specific tumor markers including α-fetoprotein were also investigated every 1–2 months. If the level of the tumor markers were increased significantly, additional dynamic CT was performed. Dynamic CT of the entire liver was performed using multidetector row helical CT (16 channels, Light Speed Ultra 16 or 64 channels, Light Speed VCT; GE, Milwaukee, WI, USA) with a 5-mm reconstructed slice width and a 5-mm slice interval. The scanning parameters were 120 kV, Auto mA (noise index, 10), 5-mm section thickness, 1.375 beam pitch, and a 0.7 or 0.4 rotation speed.

Images were obtained in four phases, which included before-contrast enhancement, early arterial, late arterial and portal venous phase after injection of 100 mL of non-ionic iodinated contrast material at a rate of 4 mL/s using an automatic injector. Hepatic arterial, portal venous and equilibrium phase scans were performed for 15–17 s, 45–47 s and 145–147 s, respectively, after triggering using an automatic bolus-tracking program. The dynamic CT appearance was evaluated using a soft-tissue window (level, 40 HU; width, 200 HU), and was confirmed following a consensus between one of the authors (T. K.) and two radiologists for each of the 67 tumors.

The dynamic CT appearance of tumor response and the relationship between tumor appearance and clinical features were evaluated from these results. In addition, local treatment results, such as the local progression-free survival rate (LPFS) and local control rate (LCR), were compared based on several evaluation methods. Treatment-related toxicities were evaluated by the Common Terminology Criteria for Adverse Events (CTCAE) ver. 4. 0.

Median follow up at the time of evaluation was 12 months (range, 6 –45).

Statistical methods

Univariate analysis using the Mantel–Haenszel χ^2-test or Student's *t*-test and multivariate analyses using the logistic regression test for comparison of statistical significance were used. The LPFS and LCR were calculated using the Kaplan–Meier method. All statistical analyses were performed using StatMate for Windows (StatMate ver. 4.01; ATMS, Tokyo, Japan). Statistical significance was defined as $P < 0.05$.

RESULTS

Dosimetric factors

THE MEDIAN GTV and PTV were 2.9 cc (range, 0.2–38.8) and 27.5 cc (range, 5.5–132.6), respectively. The median dose of PTV was 47.6 Gy (range, 39.4–60.0) and the median percentage of PTV dose relative to the isocenter dose was 98.5% (range, 95.6–102.7%) which is considered to be good dose coverage to PTV.

Dynamic CT appearance of tumor response

The dynamic CT appearance of tumor response was classified into the following four types: type 1, continuous lipiodol accumulation without early arterial enhancement (26 tumors, 38.8%) (Fig. 1); type 2, residual early arterial enhancement within 3 months after SBRT (17 tumors, 25.3%) (Fig. 2); type 3, residual early arterial enhancement more than 3 months after SBRT (19 tumors, 28.4%) (Fig. 3); and type 4, shrinking low-density area without early arterial enhancement after SBRT (five tumors, 7.5%) (Fig. 4). None of the tumors increased in size during the follow-up period. Two tumors (3.0%) demonstrated residual early arterial enhancement for more than 6 months after SBRT; however, most of these features disappeared within 6 months.

Relationship between the dynamic CT appearance of tumor response and clinical features

Table 2 presents the results of univariate analysis between the dynamic CT appearance of tumor response and clinical features, such as Child–Pugh class, sex, age, total dose, PTV, tumor location, history of resection and duration of initial treatment. *P*-value was defined as the clinical factors in each type of dynamic CT appearance as compared to those in the other types. The clinical features of patients with each of the four types of dynamic CT appearance were compared. Significant differences were observed in Child–Pugh class for type 4, sex for type 3, total dose and PTV for types 1 and 4, history of resection for type 4, and duration of initial treatment for type 2.

Table 3 presents the results of multivariate analysis between the dynamic CT appearance of tumor response and clinical features that showed significant differences in univariate analysis. History of resection in type 1 was the only significant factor in multivariate analysis.

Local treatment results

Figure 5(a,b) shows LPFS and LCR, respectively, based on the evaluation criteria 1–3 (shown below). An event was defined as local tumor progression and death in LPFS and local tumor progression in LCR; death without local tumor progression was censored. Evaluation criteria were: (1) local tumor progression defined as growth of an irradiated tumor and presence of a hypervascular nodule adjacent to the treated area; (2) local tumor progression defined as growth of an irradiated tumor, residual early arterial enhancement for more than 3 months and presence of a hypervascular nodule adjacent to the treated area; and (3) local tumor progression defined as growth of an irradiated tumor, residual early

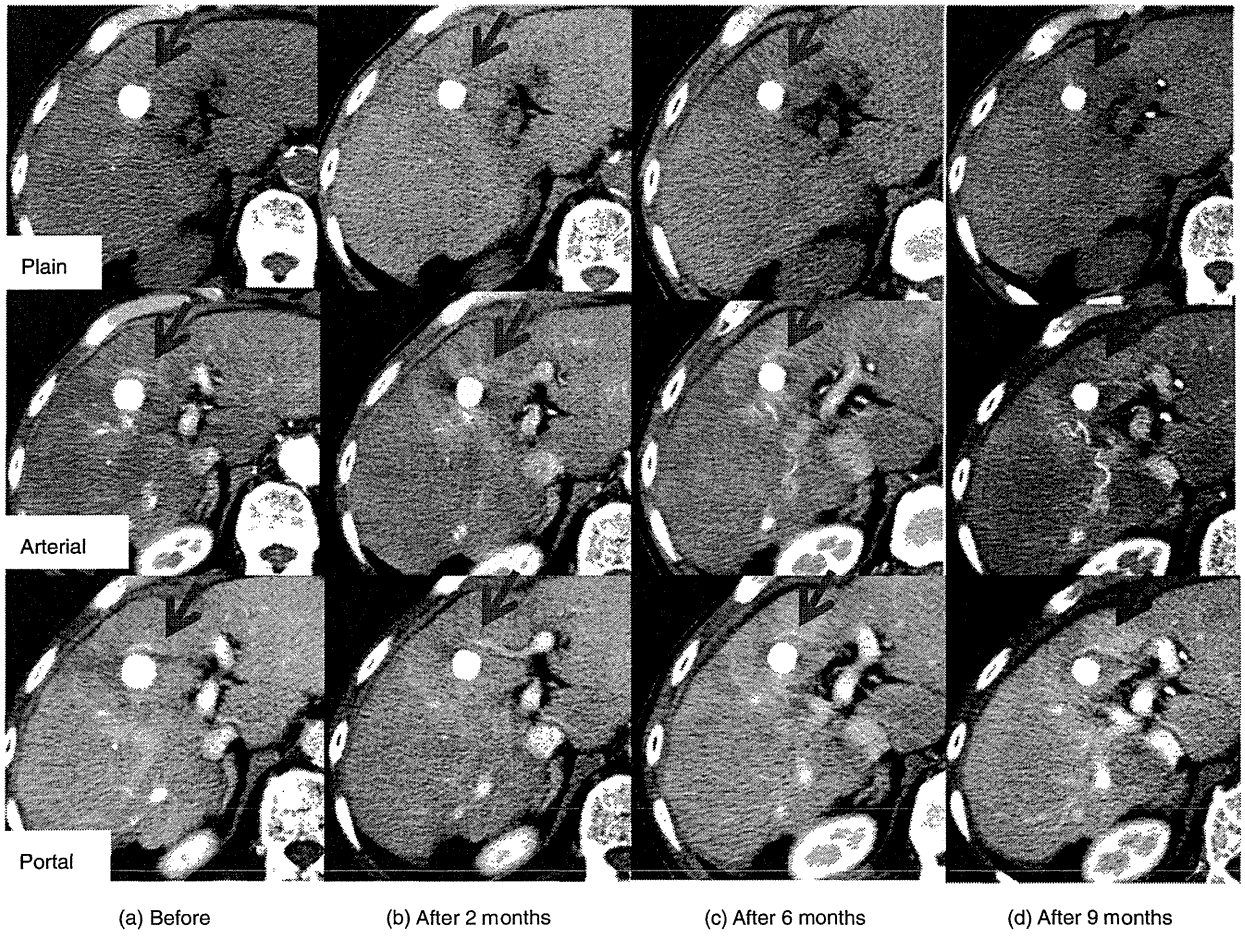

Figure 1 Dynamic computed tomography appearance of tumor response type 1 (plain, arterial and portal phase in case 37). (a) Before stereotactic body radiation therapy; (b) 2 months after; (c) 6 months after, and (d) 9 months after. Note the continuous presence of dense lipiodol accumulation without early arterial enhancement in all phases (red arrow).

arterial enhancement for more than 6 months and presence of a hypervascular nodule adjacent to the treated area.

Significant differences in LPFS were observed between evaluations 1 and 2 and between evaluations 2 and 3 ($P = 0.0089$ and 0.0242, respectively). Significant differences in LCR were observed between evaluations 1 and 2 and between evaluations 2 and 3 ($P < 0.0001$ and 0.0004, respectively).

We also evaluated the tumor response according to the Response Evaluation Criteria in Cancer of the Liver (RECICL).[12] Type 1 and 2 were equivalent to complete response (CR). Most type 3 tumors were also equivalent to CR because residual early arterial enhancement disappeared within 6 months. Two type 3 tumors demonstrated residual early arterial enhancement for more than 6 months after SBRT, however, the reduction rate of these two tumors was more than 50%, equivalent to partial response (PR). All five type 4 tumors were also equivalent to PR because of its reduction rate of more than 50%. From these results, response rate (CR + PR) was 100% and CR rate was 89.6% (60/67 tumors) according to RECICL in this study.

Treatment-related toxicities

None of the patients experienced new acute hematological or physical toxicities of more than grade 3 after TACE. However, seven patients (11.9%) developed grade 3 toxicities, such as bilirubin and ascites eleva-

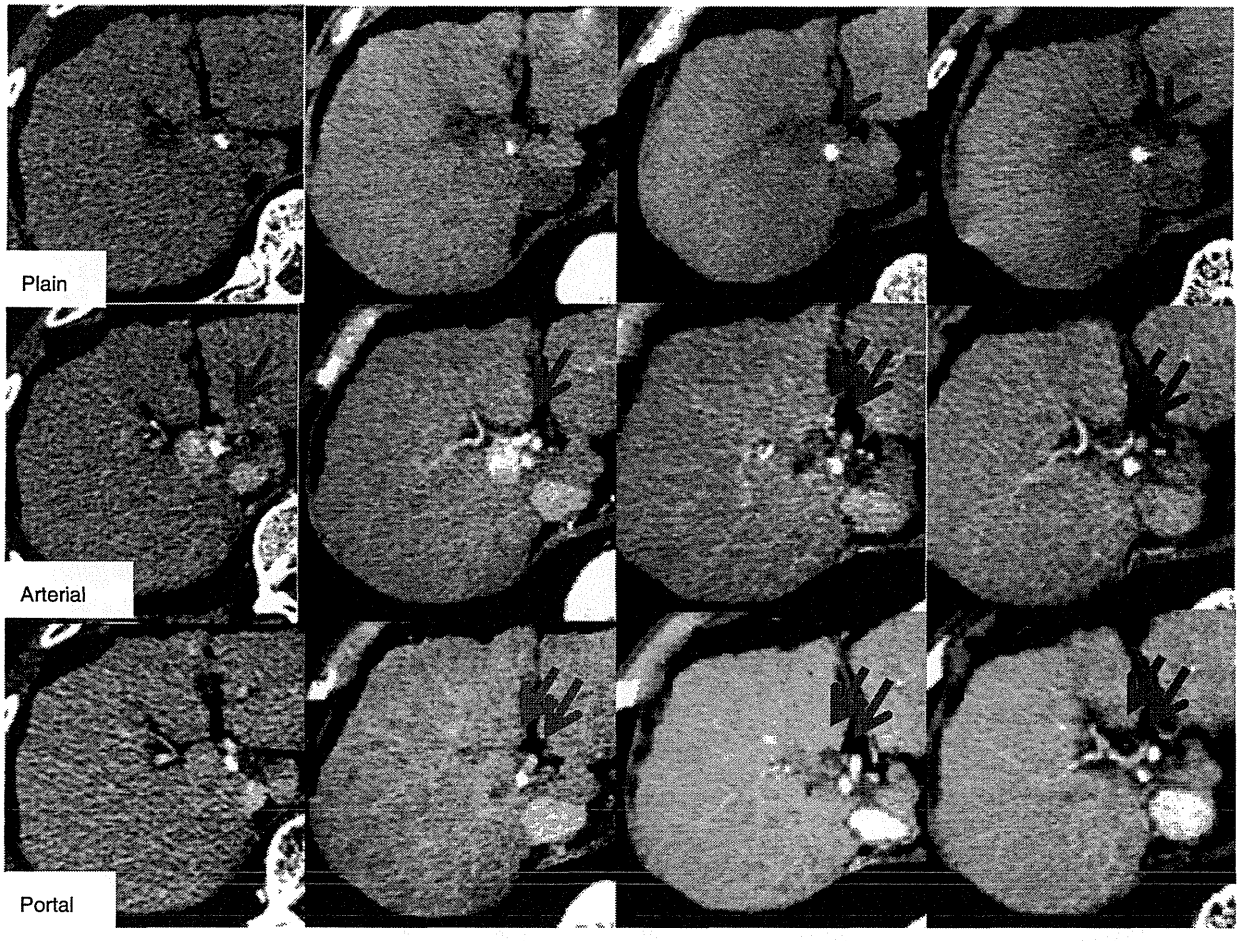

Figure 2 Dynamic computed tomography appearance of tumor response type 2 (plain, arterial and portal phase in case 9). (a) Before stereotactic body radiation therapy (SBRT); early arterial enhancement and partial residual lipiodol were observed (red arrow). (b) One month after SBRT, early arterial enhancement was still present (red arrow). Hypodensity of this tumor changed in the portal venous phase (two red arrows). (c) Three and (d) 5 months after SBRT, early arterial enhancement was no longer evident and hypodensity changed (two red arrows). Residual lipiodol accumulation is still noted (red arrow head).

tions, and one and six patients were in Child–Pugh classes A and B, respectively. None of the patients experienced RILD.

DISCUSSION

SEVERAL AUTHORS HAVE reported the typical CT appearance of RILD after SBRT; typical areas of high-dose radiation reaction appear hypodense in most non-enhanced scans and hyperdense in contrast-enhanced delayed scans.[13,14] These findings could be based on the histopathological features of veno-occlusive disease (VOD), which was recognized as radiation injury to the liver.[15,16] Olsen *et al.* described VOD with marked sinusoidal congestion and venous damage in two patients who underwent exploratory surgery following SBRT.[15] Willemart *et al.* reported that the appearance of hypodensity in the portal venous phase that becomes hyperdense in the delayed phase could be explained by decreased vascular perfusion and reduced hepatic venous drainage with subsequent stasis of the contrast medium.[16] However, the appearance of a tumor response in CT is different from that of RILD, and a tumor response after SBRT has not been reported in

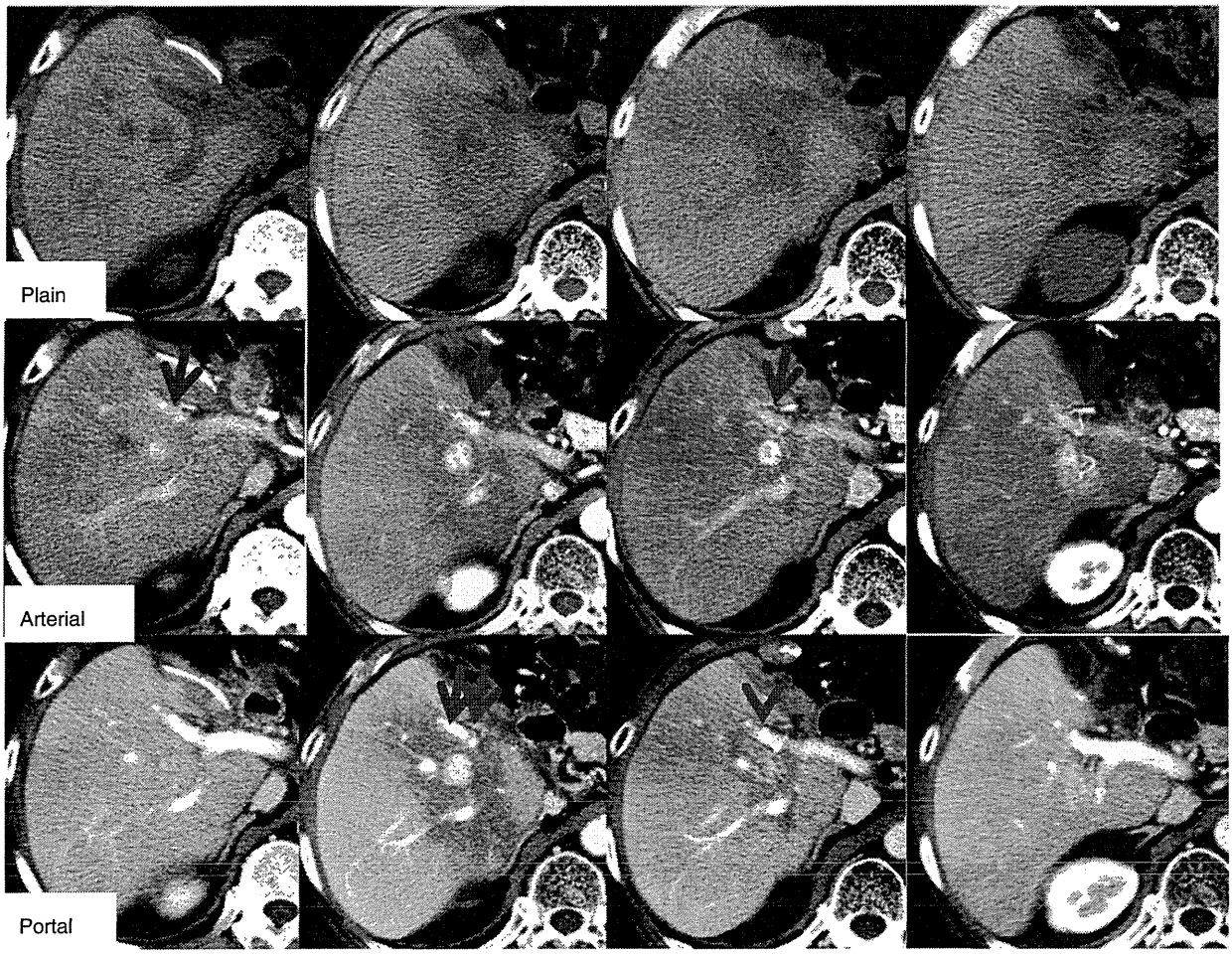

Figure 3 Dynamic computed tomography appearance of tumor response type 3 (plain, arterial and portal phase in case 39). (a) Before stereotactic body radiation therapy (SBRT), early arterial enhancement is visible (red arrow). (b) Two and (c) 6 months after SBRT, early arterial enhancement is more evident than that before SBRT in arterial (red arrow) and portal phase (two red arrows). (d) Eleven months after SBRT, although shrinking, it remains (red arrow).

detail. In this study, we classified the dynamic CT appearance of tumor response into four types. Most patients underwent TACE using lipiodol before SBRT and demonstrated a combination of residual early arterial enhancement with or without residual lipiodol. Therefore, early arterial enhancement was a characteristic dynamic CT finding for viable HCC, and the existence of residual early arterial enhancement after SBRT may indicate residual or recurrent HCC histologically.

Evaluation of the relationship between the dynamic CT appearance of tumor response and clinical features showed that history of resection in type 1 was the only significant factor in multivariate analyses. Sanuki-Fujimoto *et al.* described the CT appearance of RILD after SBRT and demonstrated that liver tissue with preserved function was more likely to be well enhanced in the delayed phase of dynamic CT.[14] However, our analysis of tumor response did not demonstrate a significant relationship between Child–Pugh class and residual early arterial enhancement observed in types 2 and 3.

Although RECIST and WHO criteria are widely used to evaluate solid tumor responses to chemotherapy or radiation therapy,[9,10] they may be inappropriate for evaluating tumor response to locoregional therapies

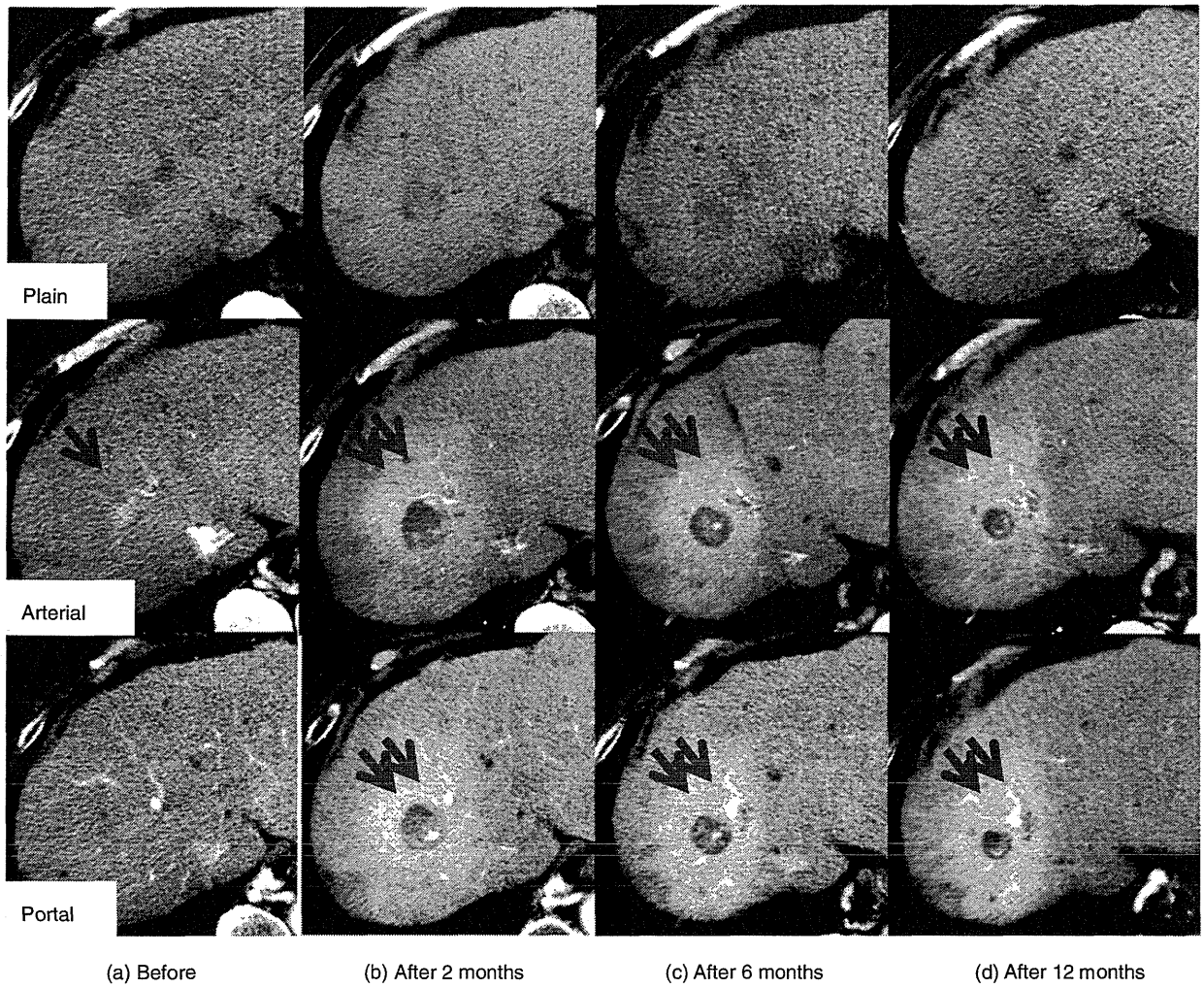

Figure 4 Dynamic computed tomography appearance of tumor response type 4 (plain, arterial and portal phase in case 11). (a) Before stereotactic body radiation therapy (SBRT), early arterial enhancement is visible (red arrow). (b) Two, (c) 6 and (d) 12 months after SBRT, hypodensity of the tumor changed and the tumor shrank without early arterial enhancement in arterial and portal phase (two red arrows). Radiation-induced liver damage is visible around the tumor.

such as ablation therapies and TACE in most patients with HCC because they only rely on tumor size reduction as a measure of effect and do not consider any necrotizing effects or tumor blood flow. RECICL were proposed by the Liver Cancer Study Group of Japan.[12] This study group addressed these concerns by including criteria that consider the biological characteristics of HCC. Tumor necrosis is regarded as a direct effect of treating a target tumor, and the dense accumulation of lipiodol is regarded as necrosis. In addition, although RECIST and WHO criteria do not specify the timing when overall treatment outcomes should be assessed, RECICL suggests that the maximum response within 3 months for TACE or local ablative therapies and 6 months for radiotherapy should be regarded as the overall treatment effects. Although the above criteria should be kept in mind for ablative therapies, which typically result in necrosis, most CT appearances after SBRT in our study did not show obvious tumor necrosis. In addition, RECICL may be inappropriate for the evaluation of tumor response by SBRT because the healing stage of ablative therapies and SBRT are different. The

Table 2 Univariate analysis between the dynamic CT appearance of tumor response and clinical features

		Type 1	*P* Uni†	Type 2	*P* Uni	Type 3	*P* Uni	Type 4	*P* Uni
Child–Pugh class	A	21	0.622	15	0.278	14	0.628	2	0.036
	B	5		2		5		3	
Sex	Male	19	0.112	11	0.731	8	0.044	3	0.955
	Female	7		6		11		2	
Age	>75 years	10	0.877	5	0.436	9	0.284	1	0.405
	≤75 years	16		12		10		4	
Total dose	>48 Gy	4	<0.001	6	0.14	3	0.415	2	0.033
	≤48 Gy	22		11		16		3	
Planning target volume	>40 cc	3	0.024	4	0.719	6	5842	5	0.0001
	≤40 cc	23		13		13		0	
Tumor location	Peripheral	24	0.082	12	0.152	15	0.729	4	0.899
	Central	2		5		4		1	
History of resection	+	10	0.877	6	0.842	5	0.242	4	0.04
	−	16		11		14		1	
Duration from first treatment	>12 months	13	0.134	14	0.038	10	0.366	4	0.37
	≤12 months	13		3		9		1	

**P*-value was defined as the clinical factors in each type of dynamic computed tomography (CT) appearance as compared to those in the other types.
†Uni: univariate analysis by the Mantel–Haenzel χ^2-test or Student's *t*-tests.

treatment results in our study were also different according to the evaluation methods, such as RECICL and our criteria including residual early arterial enhancement.

Several authors have reported treatment results of SBRT or particle therapy for HCC and their evaluation methods.[4–7] Andolino *et al.* used RECIST to evaluate tumor response after SBRT on the basis of tumor size.[4] Takeda *et al.* reported that when no tumor enhancement was detected within PTV on enhanced dynamic CT 6 months or more after SBRT, patients were considered to have no relapse.[5] With regard to particle therapies, Fukumitsu *et al.* defined local progression as growth of the irradiated tumor or the appearance of new tumors within the treatment volume after proton therapy.[6] In

Table 3 Multivariate analysis between the dynamic CT appearance of tumor response and clinical features

		Type 1	*P* Multi†	Type 2	*P* Multi	Type 3	*P* Multi	Type 4	*P* Multi
Child–Pugh class	A	21	0.999	15	0.999	14	0.999	2	0.226
	B	5		2		5		3	
Sex	Male	19	0.845	11	0.331	8	0.587	3	0.997
	Female	7		6		11		2	
Total dose	>48 Gy	4	0.505	6	0.5	3	0.999	2	0.307
	≤48 Gy	22		11		16		3	
Planning target volume	>40 cc	3	0.333	4	0.981	6	0.869	5	0.996
	≤40 cc	23		13		13		0	
History of resection	+	10	0.028	6	0.056	5	0.712	4	0.996
	−	16		11		14		1	
Duration from first treatment	>12 months	13	0.104	14	0.056	10	0.773	4	0.998
	≤12 months	13		3		9		1	

**P*-value was defined as the clinical factors in each type of dynamic computed tomography (CT) appearance as compared to those in the other types.
†Multi: multivariate logistic regression analysis.

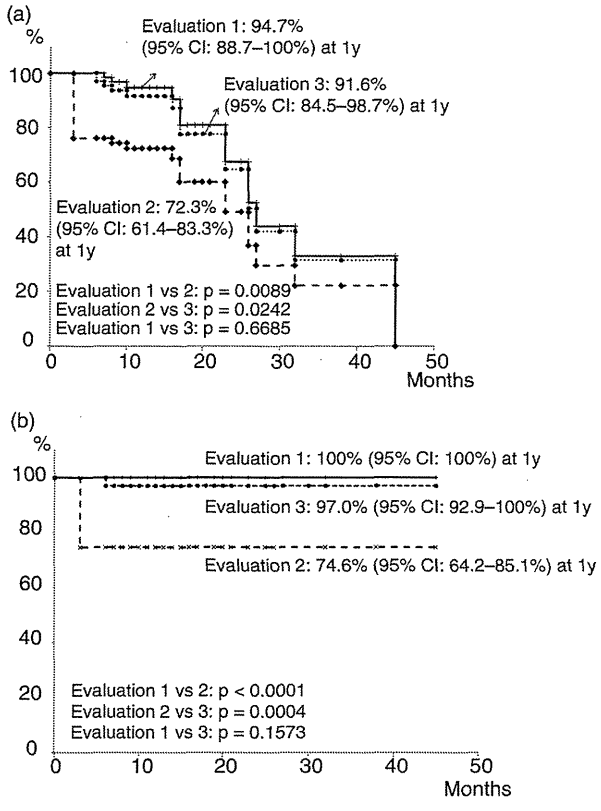

Figure 5 Treatment results of stereotactic body radiation therapy (SBRT) based on the different evaluation criteria. (a) Local progression-free survival rate (LPFS) according to evaluations 1–3. LPFS according to evaluation 2 was significantly lower than that according evaluations 1 and 3. (b) Local control rate (LCR) according to evaluations 1–3. LCR according to evaluation 2 was also significantly lower than that according to evaluation 1 and 3. CI, confidence interval; y, years.

this study, no tumors showed enlargement during the follow-up period, which should be included as a good tumor response among the other criteria described above. Takayasu *et al.* correlated histological and radiological data and indicated that accumulation of lipiodol within the tumor occurred primarily in areas of tumor necrosis.[17] They concluded that dense accumulation of lipiodol was a reliable indicator of necrosis. Based on our results, continuous dense accumulation of lipiodol without early arterial enhancement after SBRT (dynamic CT appearance, type 1) may also be included as a criterion of tumor response. However, the optimal method for evaluating early arterial enhancement after SBRT has not been confirmed. In this study, residual early arterial enhancement for more than 3 or 6 months after SBRT was observed in 19 (28.4%) and two lesions (3.0%), respectively. According to our evaluation methods (described above), residual early arterial enhancement was regarded as local progression. However, most of these findings that were noted for more than 3 months after SBRT disappeared within 6 months. We also observed shrinkage or disappearance of residual early arterial enhancement for more than 6 months after SBRT in two patients at 10 and 11 months. Our results indicate that when residual early arterial enhancement for more than 3 or 6 months was regarded as local progression, the treatment results differed significantly, especially when the treatment outcomes were assessed as early as 3 months after SBRT, which may be too early. Therefore, patient evaluation should be carefully performed. If the treated tumors are not enlarged, tumor markers are within the normal range, and residual early arterial enhancement for more than 6 months is noted, we recommend that an additional follow up should be performed, at least 12 months after SBRT. Other modalities should also be considered, such as gadoxetic acid-enhanced magnetic resonance imaging (Gd-EOB-MRI; GE Healthcare, Chalfont St. Giles, UK) or enhanced (Sonazoid; Daiichi Pharmaceutical, Tokyo, Japan) ultrasound (US) in these cases. However, in dynamic studies of Gd-EOB-MRI or Sonazoid US, appearances were similar to CT; therefore, there were few hepatocytes or Kupffer cells in the irradiated normal liver tissues, including those of HCC. Thus, it may be difficult to distinguish between tumor response and irradiated liver damage.

We recommend the following criteria for the evaluation of tumor response after SBRT with TACE based on dynamic CT appearance: (i) no tumor enlargement; (ii) continuous dense lipiodol accumulation; and (iii) disappearance of early arterial enhancement for a minimum of 6 months. However, tumors showing continuous residual early arterial enhancement should be followed up and reassessed at 12 months if no tumor enlargement is noted.

The dynamic CT scans used to study the effects of SBRT with TACE for HCC tumors had 4 patterns of response. Residual early arterial enhancement of a tumor observed 3 months after SBRT should not be considered a sign of tumor recurrence unless it persists until 6 months. Early assessment within 3 months may result in a misleading response evaluation.

Because of its retrospective nature, we are aware that this study has certain limitations, such as the low number of patients, extremely short follow-up periods,

no pathological findings for the described types of CT appearances and the effects of previous treatment. SBRT can still be considered an alternative to surgery, ablation and TACE when these therapies fail, and most of our patients had undergone those therapies previously, which possibly influenced the CT appearance of tumor responses after SBRT. We are currently planning a prospective study to address the points mentioned above.

REFERENCES

1 NCCN Clinical Practice Guidelines in Oncology (NCCN Guidelines). Hepatobiliary Cancers ver. 2. [home page on the internet]. Fort Washington, PA: National Comprehensive Cancer Network; [updated 2012 Jan 1]. Available at: http://www.nccn.org/professionals/physician_gls/f_guidelines.asp. Accessed March 12 2012

2 Thomas MB, Jaffe D, Choti MM *et al.* Hepatocellular carcinoma: consensus recommendations of the national cancer institute clinical trials planning meeting. *J Clin Oncol* 2010; **28**: 3994–4005.

3 Choi E, Rogers E, Ahmad S *et al.* Hepatobiliary cancers. In: Feig BW, Berger DH, Fuhrman GM, eds. *The M. D. Anderson Surgical Oncology Handbook*. Philadelphia, PA: Lippincott Williams &Wilkins, 2006; 320–66.

4 Andolino DL, Johnson CS, Maluccio M *et al.* Stereotactic body radiotherapy for primary hepatocellular carcinoma. *Int J Radiat Oncol Biol Phys* 2011; **81**: e447–e453.

5 Takeda A, Takahashi M, Kunieda E *et al.* Hypofractionated stereotactic radiotherapy with and without transarterial chemoembolization for small hepatocellular carcinoma not eligible for other ablation therapies: preliminary results for efficacy and toxicity. *Hepatol Res* 2008; **38**: 60–9.

6 Fukumitsu N, Sugahara S, Nakayama H *et al.* A prospective study of hypofractionated proton beam therapy for patients with hepatocellular carcinoma. *Int J Radiat Oncol Biol Phys* 2009; **74**: 831–6.

7 Kato H, Tsujii H, Miyamoto T *et al.* Results of the first prospective study of carbon ion radiotherapy for hepatocellular carcinoma with liver cirrhosis. *Int J Radiat Oncol Biol Phys* 2004; **59**: 1468–76.

8 Dawson LA. Overview: where does radiation therapy fit in the spectrum of liver cancer local – regional therapies? *Semin Radiat Oncol* 2011; **21**: 241–6.

9 Elsenhauer EA, Therasse P, Bogaerts J *et al.* New response evaluation criteria in solid tumors: revised RECIST guideline (version1.1). *Eur J Cancer* 2009; **45**: 228–47.

10 WHO. *WHO Handbook for Reporting Results of Cancer Treatment, Vol.* 48, Geneva: World Health Organization Offset Publication, 1979.

11 Kimura T, Hirokawa Y, Murakami Y *et al.* Reproducibility of organ position using voluntary breath-hold with spirometer for extracranial stereotactic radiotherapy. *Int J Radiat Oncol Biol Phys* 2004; **60**: 1307–13.

12 Kudo M, Kubo S, Takayasu K *et al.* Response Evaluation Criteria in Cancer of the Liver (RECICL) proposed by the Liver Cancer Study Group of Japan (2009 Revised Version). *Hepatol Res* 2010; **40**: 686–92.

13 Wulf J, Herfarth KK. Normal tissue dose constraints in stereotactic body radiation therapy for liver tumors. Stereotactic Body Radiation Therapy. In: Kavanagh BD, Timmerman RD, eds. *Stereotactic Body Radiation Therapy*. Philadelphia: Lippincott Williams & Wilkins, 2005; 39–45.

14 Sanuki-Fujimoto N, Takeda A, Ohashi T *et al.* CT evaluations of focal liver reactions following stereotactic body radiotherapy for small hepatocellular carcinoma with cirrhosis: relationship between imaging appearance and baseline liver function. *Br J Radiol* 2010; **83**: 1063–71.

15 Olsen CC, Welsh J, Kavanagh BD *et al.* Microscopic and macroscopic tumor and parenchymal effects of liver stereotactic body radiotherapy. *Int J Radiat Oncol Biol Phys* 2009; **73**: 1414–24.

16 Willemart S, Nicaise N, Struyven J, Van Gansbeke D. Acute radiation-induced hepatic injury: evaluation by triphasic contrast enhanced helical CT. *BJR* 2000; **73**: 544–6.

17 Takayasu K, Arii S, Matsuo N *et al.* Comparison of CT findings with resected specimens after chemoembolization with iodized oil for hepatocellular carcinoma. *AJR Am J Roentgenol* 2000; **175**: 699–704.

International Journal of
Radiation Oncology
biology • physics

www.redjournal.org

Clinical Investigation: Gynecologic Cancer

Dose-Volume Histogram Predictors of Chronic Gastrointestinal Complications After Radical Hysterectomy and Postoperative Concurrent Nedaplatin-Based Chemoradiation Therapy for Early-Stage Cervical Cancer

Fumiaki Isohashi, MD, PhD,* Yasuo Yoshioka, MD, PhD,* Seiji Mabuchi, MD, PhD,† Koji Konishi, MD, PhD,* Masahiko Koizumi, MD, PhD,*,‡ Yutaka Takahashi, PhD,*,‡ Toshiyuki Ogata, PhD,*,‡ Shintaroh Maruoka, MD,* Tadashi Kimura, MD, PhD,† and Kazuhiko Ogawa, MD, PhD*

*Departments of *Radiation Oncology and †Obstetrics and Gynecology, ‡Division of Medical Physics, Oncology Center, Osaka University Hospital, Suita, Osaka, Japan*

Received Jan 24, 2012, and in revised form May 1, 2012. Accepted for publication May 10, 2012

Summary

In this study, dose-volume histogram parameters of the small bowel loops were predictive for the development of chronic gastrointestinal (GI) complications after postoperative concurrent nedaplatin-based chemoradiation therapy for early-stage cervical cancer. Multivariate analysis indicated that V40 (volume receiving more than 40 Gy) of the small bowel loops and smoking were independent predictors of GI complications.

Purpose: The purpose of this study was to evaluate dose-volume histogram (DVH) predictors for the development of chronic gastrointestinal (GI) complications in cervical cancer patients who underwent radical hysterectomy and postoperative concurrent nedaplatin-based chemoradiation therapy.

Methods and Materials: This study analyzed 97 patients who underwent postoperative concurrent chemoradiation therapy. The organs at risk that were contoured were the small bowel loops, large bowel loop, and peritoneal cavity. DVH parameters subjected to analysis included the volumes of these organs receiving more than 15, 30, 40, and 45 Gy (V15-V45) and their mean dose. Associations between DVH parameters or clinical factors and the incidence of grade 2 or higher chronic GI complications were evaluated.

Results: Of the clinical factors, smoking and low body mass index (BMI) (<22) were significantly associated with grade 2 or higher chronic GI complications. Also, patients with chronic GI complications had significantly greater V15-V45 volumes and higher mean dose of the small bowel loops compared with those without GI complications. In contrast, no parameters for the large bowel loop or peritoneal cavity were significantly associated with GI complications. Results of the receiver operating characteristics (ROC) curve analysis led to the conclusion that V15-V45 of the small bowel loops has high accuracy for prediction of GI complications. Among these parameters, V40 gave the highest area under the ROC curve. Finally, multivariate analysis was performed with V40 of the small bowel loops and 2 other clinical parameters that were judged to be potential risk factors for chronic GI complications: BMI and smoking. Of these 3 parameters, V40 of the small bowel loops and smoking emerged as independent predictors of chronic GI complications.

Reprint requests to: Fumiaki Isohashi, Department of Radiation Oncology, Osaka University Graduate School of Medicine, 2-2 (D10) Yamadaoka, Suita, Osaka 565-0871, Japan. Tel: (+81) 6-6879-3482; Fax: (+81) 6-6879-3489; E-mail: isohashi@radonc.med.osaka-u.ac.jp

Conflict of interest: none.

Int J Radiation Oncol Biol Phys, Vol. 85, No. 3, pp. 728–734, 2013
0360-3016/$ - see front matter
doi:10.1016/j.ijrobp.2012.05.021

Conclusions: DVH parameters of the small bowel loops may serve as predictors of grade 2 or higher chronic GI complications after postoperative concurrent nedaplatin-based chemoradiation therapy for early-stage cervical cancer. © 2013 Elsevier Inc.

Introduction

Adjuvant whole-pelvic radiation therapy (RT) after radical hysterectomy reduces locoregional recurrence in cervical cancer patients after surgery with adverse risk factors (1, 2). However, patients undergoing whole-pelvic RT after radical hysterectomy may suffer severe gastrointestinal (GI) complications with an incidence varying from 3%-13% for patients treated with pelvic RT alone (1-3). Moreover, while adjuvant concurrent chemoradiation therapy has been shown in several studies to improve survival rates for high-risk cervical cancer patients compared with adjuvant RT alone, GI complications were observed more frequently in conjunction with concurrent chemoradiation therapy than with RT alone (4). Therefore it is important to improve the feasibility of adjuvant concurrent chemoradiation therapy by reducing GI complications.

Because the small bowel is one of the critical organs involved in GI complications, a predictive model of acute GI complications of the small bowel has been established with the aid of Quantitative Analyses of Normal Tissue Effects in the Clinic (QUANTEC) (5). However, the correlation between dose-volume effect and chronic GI complications of the small bowel has not been extensively investigated.

Since 2000, we have been using postoperative concurrent nedaplatin-based chemoradiation therapy for early-stage cervical cancer patients with adverse risk factors (6). The purpose of the study reported here was to evaluate dose-volume histogram (DVH) predictors for the development of chronic GI complications in cervical cancer patients who underwent radical hysterectomy and postoperative concurrent nedaplatin-based chemoradiation therapy.

Methods and Materials

Patients

A total of 131 patients with cervical cancer received radical hysterectomy and postoperative RT at our institute between April 2000, when we started to use postoperative concurrent nedaplatin-based chemoradiation therapy, and September 2010. Treatment criteria for postoperative RT were previously described (6, 7). Thirty-four of these patients were excluded from the study: 18 who received extended-field radiation therapy alone because of multiple lymph node metastases (7), 9 who refused concurrent chemotherapy, 3 who received intracavitary brachytherapy with whole-pelvic RT because of a close surgical margin, and 4 early patients who did not undergo radiation treatment planning computed tomography (CT) with a 2-dimensional (2D) era. The remaining 97 patients treated with concurrent chemoradiation therapy were analyzed for this study with a minimum follow-up period of 3 months. This study was approved by our institutional review board.

Radiation therapy and chemotherapy

Whole-pelvic RT was delivered with 2D planning in 65 patients between April 2000 and March 2008 and with 3-dimensional (3D) conformal treatment planning in 32 patients starting April 2008. During the 2D era, RT was delivered using 10-megavolt X rays from a linear accelerator with the anteroposterior parallel opposing technique. The superior margin of the whole-pelvic RT was at the upper edge of the fifth lumbar vertebra and the inferior margin was the inferior edge of the obturator foramen. Laterally, the field extended 2 cm beyond the lateral margins of the bony pelvic wall. After we defined an isocenter or field-shape in the X-ray simulator, CT with the isocenter position marked was performed with 5.0-mm slices without filling the bladder to calculate the monitor unit and check the dose distribution. The CT scan range was from the upper edge of L3 to at least 7 cm below the bottom of the obturator foramen. The dose distribution was calculated using a commercial treatment planning system (FOCUS; Elekta, Stockholm Sweden). The prescribed RT doses were 50 Gy administered in 25 fractions over 5 weeks at the center of the body. Multileaf collimators were used to block the upper and lower corners of the radiation field. No target volume or organ at risk was delineated before treatment. Since April 2008, all patients have been treated with 3D conformal treatment planning. RT planning CT was performed with 2.5-mm slices with normal quiet breathing and a full-bladder scan. The CT scan range was the same as that used in 2D planning. A commercial treatment planning system (XiO TPS; Elekta) was used to design the radiation fields. The clinical target volume (CTV) comprised a central vaginal CTV and a regional nodal CTV. The former included the proximal vagina and paravaginal tissues and the latter consisted of the common iliac, external and internal iliac, and presacral lymph nodes. CTVs were contoured according to the consensus guidelines of the Radiation Therapy Oncology Group (RTOG) 0418 (8) and its atlas on the RTOG website. The planning target volume (PTV) was generated by using 1.0-cm uniform expansion of the CTV. The prescribed RT doses were 50 Gy at the center of the PTV, administered in 25 fractions over 5 weeks by means of the 3D 4-field box technique. Multileaf collimators were used to cover the PTV with a margin of approximately 5 mm. No organ at risk was delineated before treatment. Nedaplatin (40 mg/m^2) was given intravenously on a weekly basis during the course of whole-pelvic RT for 5 weeks as previously described (6).

Contouring and evaluation of normal structures

The organs at risk that were contoured comprised the small bowel loops, large bowel loop, and peritoneal cavity. All contouring was done retrospectively. The superior and inferior extents of critical organs were outlined on all CT slices containing portions of the PTV (3D) or field margins (2D), including an additional area 2-cm superior and inferior to the limit of the PTV or field margins. Therefore, the organs at risk, including the large bowel loop, small bowel loops, and peritoneal cavity, could not be contoured in full volume. The large bowel loop was contoured first as a single loop continuing from the end of the sigmoid colon to the ascending colon, and the remaining bowel loops were classified as the small bowel loops. A preoperative diagnostic CT scan using oral and intravenous contrast media was performed in 92/97 patients (95%). This preoperative CT scan

was displayed when the organs at risk were contoured using postoperative radiation treatment planning CT. Diagnostic CT images were not fused to the planning scans. In the remaining 5 patients, postoperative radiation treatment planning CT only was used for contouring of the organs at risk. The peritoneal cavity was defined as including the volume surrounding the small bowel loops out to the edge of the peritoneum. The boundaries included the abdominal wall anteriorly and anterolaterally, the retroperitoneal and deep pelvic muscles posterolaterally, and the great vessels, vertebral bodies, and sacrum posteriorly. The rectum and bladder were excluded from the peritoneal cavity volume. DVH parameters subjected to analysis included the mean doses to the small bowel loops, large bowel loop, and peritoneal cavity, and the volumes of these organs receiving more than 15, 30, 40, and 45 Gy (V15-V45).

Follow-up and evaluation of chronic GI complications

The patients were followed up by gynecologic and radiation oncologists on an outpatient basis every month in the first year, every 2 months in the second year, every 3 months in the third year, every 4 months in the fourth year, every 6 months in the fifth year, and annually thereafter until 10 years after treatment. We defined a chronic complication as a GI event that occurred more than 3 months after radiation therapy was started. The severity of the GI complication was classified according to the RTOG/European Organization for Research and Treatment of Cancer Late Radiation Morbidity Score. Toxicity data including the grade of GI complications were collected retrospectively through hospitalization and follow-up records.

Statistical analysis

Associations between selected DVH parameters (V15, V30, V40, V45, and mean dose) and the incidence of grade 2 or higher chronic GI complications were evaluated. The relationships between clinical or DVH parameters and the incidence of chronic GI complications were analyzed with the Mann-Whitney U test for quantitative variables and the Fisher exact test for categorical variables. The mean DVH parameters for the small bowel loops, large bowel loop, and peritoneal cavity of patients with and without GI complications were compared by Mann-Whitney U test. Receiver operating characteristics (ROC) curve analysis of each of the DVH parameters was performed to select the most relevant threshold for prediction of a grade 2 or higher chronic GI complication. The predictive value of a parameter was evaluated based on the area under the ROC curve (AUC). The AUC reflects the ability of the test to distinguish between patients with and without disease. The optimal threshold for each DVH parameter was defined as the point yielding the minimal value for $(1 - \text{sensitivity})^2 + (1 - \text{specificity})^2$, which is the point on the ROC curve closest to the upper left-hand corner (9). Multivariate analysis using Cox regression models was performed to identify risk factors associated with grade 2 or higher chronic GI complications. The actuarial incidence of GI complications was calculated with the Kaplan-Meier method and differences between groups were compared by log-rank test. A P value of $<.05$ or a 95% confidence interval not encompassing 1 was considered to be statistically significant. All statistical tests were 2-sided.

Results

The characteristics of the 97 patients are shown in Table 1. The median follow-up period from the start of radiation therapy was 43 months (range 4-111 months). None of the patients experienced a local or distant recurrence within 3 months. The Eastern Cooperative Oncology Group performance status was 0-1 for all patients. The median age of the patients was 51 years old (range 28-70 years old). Twenty-three patients (24%) had a history of smoking, with a median Brinkman index (number of cigarettes per day × smoking years) of 400 (range 100-1200). The median total dose of nedaplatin was 285 mg (range 30-375 mg). Ninety-two patients (95%) received the whole RT dose as planned (50 Gy), but 3 patients (3%) received only 46 Gy and 2 (2%) received 44 Gy because of neutropenia (4 patients) or patient refusal (1 patient). Eighty-one patients (84%) had grade 0-1, 6 (6%) had grade 2, and 10 (10%) had grade 3 chronic GI

Table 1 Patient and treatment characteristics

	No. (%)
Age (y)	
Mean	51
SD	±10
T-stage	
T1	53 (55)
T2	44 (45)
N-stage	
N0	64 (66)
N1	33 (34)
Histology	
SCC	71 (73)
Ad	24 (25)
Others	2 (2)
Smoking	
None	74 (76)
Yes	23 (24)
Diabetes	
None	94 (97)
Yes	3 (3)
Abdominopelvic surgery	
None	94 (97)
Yes	3 (3)
BMI (kg/m^2)	
Mean	21.6
SD	±3.8
RT total dose (Gy)	
50	92 (95)
46	3 (3)
44	2 (2)
RT technique	
2D	65 (67)
3D	32 (33)
Total nedaplatin (mg)	
Mean	274
SD	±52

Abbreviations: 2D = 2-dimensional; 3D = 3-dimensional; Ad = adenocarcinoma; BMI = body mass index; RT = radiation therapy; SCC = squamous cell carcinoma; SD = standard deviation.

Table 2 Univariate analysis (Mann-Whitney *U* test and Fisher exact test) for the development of grade 2 or higher chronic GI complications

Variable	Grade 0-1 No.	Grade 2-3 No.	*P* value
Age (y)			
<52	39	10	.294
≥52	42	6	
Total nedaplatin (mg)			
<285	39	8	.892
≥285	42	8	
T-stage			
T1	46	7	.338
T2	35	9	
N-stage			
N0	53	11	.798
N1	28	5	
Histology			
SCC	60	11	.660
Non-SCC	21	5	
RT total dose			
50 Gy	76	16	.308
<50 Gy	5	0	
RT technique			
2D	57	8	.133
3D	24	8	
Smoking			
None	66	8	.005
Yes	15	8	
BMI (kg/m^2)			
<22	43	14	.011
≥22	38	2	

Abbreviations: 2D = 2-dimensional; 3D = 3-dimensional; BMI = body mass index; GI = gastrointestinal; RT = radiation therapy; SCC = squamous cell carcinoma.

Table 3 Comparison of mean DVH parameters of the small bowel loops, large bowel loop, and peritoneal cavity in patients with and without chronic GI complications (Mann-Whitney *U* test)

	Overall	Grade 0-1	Grade 2-3	*P* value
		Small bowel loops		
		Mean volume ± SE (mL)		
V15	337 ± 15	299 ± 13	527 ± 37	<.001
V30	308 ± 13	273 ± 11	485 ± 29	<.001
V40	289 ± 13	255 ± 11	458 ± 27	<.001
V45	280 ± 12	247 ± 11	444 ± 26	<.001
		Mean dose (cGy ± SE)		
	3,523 ± 80	3,429 ± 86	3,994 ± 160	<.001
		Large bowel loop		
		Mean volume ± SE (mL)		
V15	241 ± 12	241 ± 12	239 ± 34	.730
V30	207 ± 10	210 ± 11	192 ± 23	.550
V40	183 ± 10	189 ± 11	156 ± 17	.331
V45	176 ± 9	182 ± 10	149 ± 16	.321
		Mean dose (cGy ± SE)		
	2,747 ± 62	2,768 ± 66	2,639 ± 174	.487
		Peritoneal cavity		
		Mean volume ± SE (mL)		
V15	1,151 ± 29	1,129 ± 32	1,262 ± 70	.111
V30	1,045 ± 25	1,027 ± 27	1,138 ± 64	.174
V40	974 ± 25	960 ± 27	1,049 ± 65	.336
V45	941 ± 24	927 ± 26	1,013 ± 65	.343
		Mean dose (cGy ± SE)		
	3,421 ± 47	3,387 ± 50	3,596 ± 122	.169

Abbreviations: DVH = dose-volume histogram; GI = gastrointestinal; SE = standard error; V15-45 = volume receiving more than respective dose.

complications. Of the 10 patients with grade 3 GI complications, 5 (5% of all patients) had small bowel obstruction requiring surgery.

The incidence of chronic GI complications was analyzed as a function of clinical factors. Because there were few patients with diabetes or a history of abdominopelvic surgery among the study population, we did not analyze these factors. The results of univariate analyses are shown in Table 2. Smoking habit and low body mass index (BMI; <22) were significantly associated with grade 2 or higher GI complications. The mean DVH parameters of the small bowel loops, large bowel loop, and peritoneal cavity of patients with and without GI complications are shown in Table 3. Patients with grade 2 or higher GI complications had significantly greater V15-V45 volumes in the small bowel loops than did those without GI complications ($P<.001$). The mean dose to the small bowel loops differed significantly for patients with and without GI complications (39.94 vs 34.29 Gy, $P<.001$). In contrast, none of the parameters for the large bowel loop or peritoneal cavity were significantly associated with GI complications.

ROC curve analysis was performed to select the most relevant parameter to identify predictors of grade 2 or higher chronic GI complications among DVH parameters for the small bowel loops. The results are shown in Table 4. Because AUCs for mean dose, V15, V30, V40, and V45 were 0.693, 0.909, 0.912, 0.921, and 0.890, respectively, indicating that V15-V45 have good accuracy for prediction of GI complications. Strong collinearity among V15-V45 was expected in multivariate

Table 4 ROC curve analysis for DVH parameters of small bowel loops in relation to grade 2 or higher chronic GI complications

	AUC	95% CI	Optimal threshold Value	Sensitivity/specificity (%)
Mean dose	0.693	0.580-0.806	3600 cGy	62.5/62.5
V15	0.909	0.855-0.963	380 mL	93.8/82.1
V30	0.912	0.857-0.967	360 mL	93.8/82.1
V40	0.921	0.869-0.972	340 mL	87.5/87.2
V45	0.890	0.819-0.962	340 mL	87.5/85.1

Abbreviations: AUC = area under the ROC curve; CI = confidence interval; DVH = dose-volume histogram; GI = gastrointestinal; ROC = receiver operating characteristics; V15-45 = volume receiving more than respective dose.

Table 5 Multivariate analysis for the development of grade 2 or higher chronic GI complications

Variable	HR (95% CI)	*P* value
V40 of small bowel loops (mL)	1.012 (1.007-1.018)	<.001
BMI (<22 vs >22)	3.024 (0.585-15.622)	.187
Smoking (yes vs no)	3.103 (1.023-9.415)	.046

Abbreviations: BMI = body mass index; CI = confidence interval; GI = gastrointestinal; HR = hazard ratio; V40 = volume receiving more than 40 Gy.

analysis. Therefore, we used V40 of the small bowel loops in multivariate analysis because this parameter had the highest AUC value. The optimal threshold for V40 was 340 mL. Thus, multivariate analysis was performed with V40 of the small bowel loops and 2 other clinical parameters that were judged to be potential risk factors for chronic GI complications: BMI and smoking habit. Of these 3 parameters, V40 of the small bowel loops and smoking emerged as independent predictors of GI complications (Table 5).

The overall incidences of grade 2 or higher GI complications were 0% (0/39), 7% (2/29), and 48% (14/29) for patients with V40 values of <250 mL, 250-340 mL, and >340 mL, respectively. Thus, the overall incidence of grade 2 or higher GI complications increased in a volume-dependent manner. Therefore, we performed Kaplan-Meier estimates of the cumulative incidence curves for grade 2 or higher chronic GI complications stratified by V40 of the small bowel loops using the above intervals. The cumulative incidence curves for grade 2 or higher chronic GI complications stratified by V40 of the small bowel loops are shown in Fig. The 3-year cumulative incidences of grade 2 or higher GI complications were 0%, 8.4%, and 46.2% for patients with V40 values of <250 mL, 250-340 mL, and >340 mL, respectively, with a significantly higher risk for patients with V40 > 340 mL than for the other groups ($P<.001$).

Discussion

Several previous studies have introduced predictive factors potentially associated with chronic GI complications after RT for gynecologic malignancies employing several types of therapy (3, 10-14). These factors include total RT dose, RT dose per fraction, history of diabetes, acute toxicity, BMI, age, previous abdominopelvic surgery, and smoking. In our study, smoking and low BMI were identified by univariate analysis as predictors of GI complications. Moreover, the V15-V45 volumes and the mean dose of the small bowel loops all showed a significant association with chronic GI complications. In addition, multivariate analysis identified V40 of the small bowel loops and smoking as independent predictors of GI complications. To the best of our knowledge, ours is the first study to show that DVH parameters of the small bowel loops derived with an up-to-date approach are associated with chronic GI complications after postoperative concurrent chemoradiation therapy for cervical cancer.

We believe that our findings are important for the practice of the radiation oncology, because adverse events caused by radiation exposure, such as GI complications, may be relieved by using an appropriate radiation technique or a mechanical device such as a belly-board. Recently, intensity modulated radiation therapy (IMRT) has emerged as a sophisticated technique for treatment of tumor regions or areas at risk of recurrence, while sparing adjacent normal tissue from high-dose irradiation, including in patients with gynecological cancer treated with IMRT after radical hysterectomy (15-18).

Two methods for contouring the small bowel volume have been reported: one uses direct delineation of the individual loops, whereas the other bases delineation on the peritoneal cavity because the bowel may lie within this space at any time throughout the course of treatment (5). Because these methods have not been compared to determine which leads to better predictions of chronic complications of the small bowel, we established separate parameters for the irradiated volume of the small bowel loops and the peritoneal cavity to examine which parameters correlated with

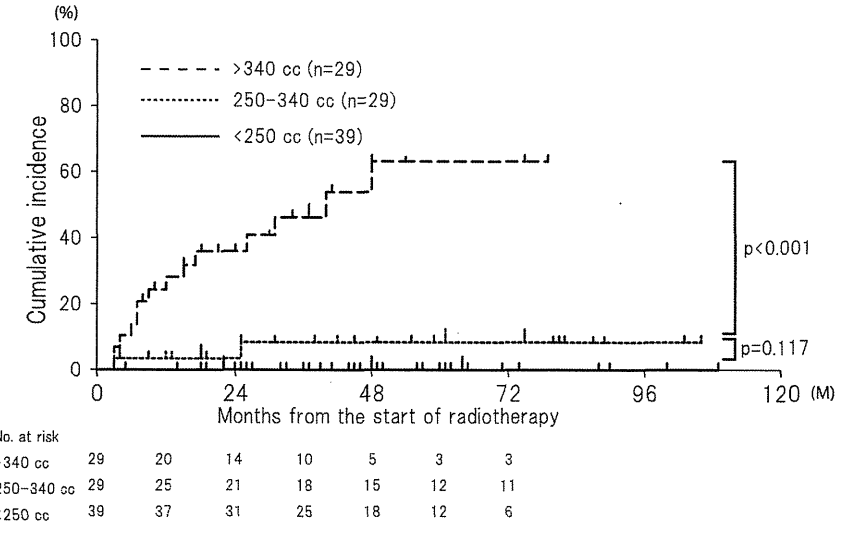

Fig. Kaplan-Meier estimates of cumulative incidence curves for grade 2 or higher chronic gastrointestinal (GI) complications stratified by V40 of the small bowel loops. The 3-year cumulative incidences of grade 2 or higher GI complications were 0%, 8.4%, and 46.2% for patients with V40 values of <250 mL, 250-340 mL, and >340 mL, respectively, with a significantly higher risk for patients with V40 > 340 mL than for the other groups (log-rank test; $P<.001$).

development of chronic GI complications. Interestingly, patients with grade 2 or higher chronic GI complications featured significantly higher V15-V45 volumes and mean dose to the small bowel loops than did patients without this feature. In contrast, none of the parameters for the peritoneal cavity showed any association with chronic GI complications. Similarly, parameters for the large bowel did not correlate with radiation-induced chronic GI complications. These findings suggest that, compared to the peritoneal cavity, the small bowel loops may constitute a better predictor of chronic GI complications. However, it is also likely that the dose to the peritoneal cavity will be a predictor of acute GI complications (5), and Wedlake et al found that cumulative acute GI symptoms, measured using the questionnaire, are associated with consequential late symptoms (14). Collectively, these results suggest that our finding that parameters for the small bowel loops are better predictors of chronic GI complication, compared with those for the peritoneal cavity, requires verification in larger prospective studies.

The findings in this study should be interpreted with an understanding of the following limitations. First, the heterogeneity in the treatment planning approach over the period of the study (2D vs 3D), the low number of events, and the lack of a prespecified model or protocol are important limitations of the data and analysis. Second, our method resulted in large uniform doses to regions of the small bowel, which differ from the dose patterns produced by techniques such as IMRT, which is becoming more prevalent. Therefore, we cannot exclude the possibility that the optimal DVH parameter predictors found in this study may differ from those for IMRT.

Additionally, we used weekly nedaplatin as concurrent chemotherapy, whereas chemoradiation therapy with 40 mg/m^2 of weekly cisplatin is now accepted as a standard first-line treatment. We therefore cannot exclude the possibility that the optimal DVH parameter predictors found in the study may be chemotherapy-type specific. Furthermore, the small bowel DVH parameters were estimated based on only 1 radiation treatment planning CT before RT, while in fact daily variability of the distention or movement of the small bowels during the treatment course may have affected the dose-volume profile. Also, especially in the 2D era, radiation treatment planning CT performed with 5.0-mm slices without filling the bladder may not reflect the actual dose received. Han et al reported that the dose distribution in the small bowel as observed on CT varies significantly from week to week because of the interfractional variations of small-bowel positions (19). In addition, image guided RT is now widely used in many institutions (20). Therefore, further studies using image guided RT will be necessary to investigate the influence of intra- and interfraction motion of the small bowel loops on chronic GI complications.

Within these limitations, we conclude that DVH parameters of the small bowel loops may serve as predictors of chronic GI complications of grade 2 or higher after postoperative concurrent nedaplatin-based chemoradiation therapy in early-stage cervical cancer patients. For these patients, we recommend that V40 of the small bowel loops should be <340 mL to avoid chronic GI complications using a conventional 2D or 3D technique.

References

1. Sedlis A, Bundy BN, Rotman MZ, Lentz SS, Muderspach LI, Zaino RJ. A randomized trial of pelvic radiation therapy versus no further therapy in selected patients with stage IB carcinoma of the cervix after radical hysterectomy and pelvic lymphadenectomy: a Gynecologic Oncology Group Study. *Gynecol Oncol* 1999;73: 177-183.
2. Fiorica JV, Roberts WS, Greenberg H, Hoffman MS, LaPolla JP, Cavanagh D, et al. Morbidity and survival patterns in patients after radical hysterectomy and postoperative adjuvant pelvic radiotherapy. *Gynecol Oncol* 1990;36:343-347.
3. Chen SW, Liang JA, Yang SN, Hung YC, Yeh LS, Shiau AC, et al. Radiation injury to intestine following hysterectomy and adjuvant radiotherapy for cervical cancer. *Gynecol Oncol* 2004;95: 208-214.
4. Peters WA 3rd, Liu PY, Barrett RJ 2nd, Stock RJ, Monk BJ, Berek JS, et al. Concurrent chemotherapy and pelvic radiation therapy compared with pelvic radiation therapy alone as adjuvant therapy after radical surgery in high-risk early-stage cancer of the cervix. *J Clin Oncol* 2000;18:1606-1613.
5. Kavanagh BD, Pan CC, Dawson LA, Das SK, Li XA, Ten Haken RK, et al. Radiation dose-volume effects in the stomach and small bowel. *Int J Radiat Oncol Biol Phys* 2010;76(Suppl. 3):S101-S107.
6. Mabuchi S, Morishige K, Isohashi F, Yoshioka Y, Takeda T, Yamamoto T, et al. Postoperative concurrent nedaplatin-based chemoradiotherapy improves survival in early-stage cervical cancer patients with adverse risk factors. *Gynecol Oncol* 2009;115:482-487.
7. Mabuchi S, Okazawa M, Isohashi F, Ohta Y, Maruoka S, Yoshioka Y, et al. Postoperative whole pelvic radiotherapy plus concurrent chemotherapy versus extended-field irradiation for early-stage cervical cancer patients with multiple pelvic lymph node metastases. *Gynecol Oncol* 2011;120:94-100.
8. Small W Jr., Mell LK, Anderson P, Creutzberg C, De Los Santos J, Gaffney D, et al. Consensus guidelines for delineation of clinical target volume for intensity-modulated pelvic radiotherapy in postoperative treatment of endometrial and cervical cancer. *Int J Radiat Oncol Biol Phys* 2008;71:428-434.
9. Akobeng AK. Understanding diagnostic tests 3: receiver operating characteristic curves. *Acta Paediatr* 2007;96:644-647.
10. Iraha S, Ogawa K, Moromizato H, Shiraishi M, Nagai Y, Samura H, et al. Radiation enterocolitis requiring surgery in patients with gynecological malignancies. *Int J Radiat Oncol Biol Phys* 2007;68: 1088-1093.
11. Kasuya G, Ogawa K, Iraha S, Nagai Y, Shiraishi M, Hirakawa M, et al. Severe late complications in patients with uterine cancer treated with postoperative radiotherapy. *Anticancer Res* 2011;31: 3527-3533.
12. Eifel PJ, Jhingran A, Bodurka DC, Levenback C, Thames H. Correlation of smoking history and other patient characteristics with major complications of pelvic radiation therapy for cervical cancer. *J Clin Oncol* 2002;20:3651-3657.
13. Kizer NT, Thaker PH, Gao F, Zighelboim I, Powell MA, Rader JS, et al. The effects of body mass index on complications and survival outcomes in patients with cervical carcinoma undergoing curative chemoradiation therapy. *Cancer* 2011;117:948-956.
14. Wedlake LJ, Thomas K, Lalji A, Blake P, Khoo VS, Tait D, et al. Predicting late effects of pelvic radiotherapy: is there a better approach? *Int J Radiat Oncol Biol Phys* 2010;78:1163-1170.
15. Roeske JC, Lujan A, Rotmensch J, Waggoner SE, Yamada D, Mundt AJ. Intensity-modulated whole pelvic radiation therapy in patients with gynecologic malignancies. *Int J Radiat Oncol Biol Phys* 2000;48:1613-1621.
16. Jhingran A, Winter K, Portelance L, Miller BE, Salehpour M, Gaur R, et al. A phase II study of intensity modulated radiation therapy (IMRT) to the pelvic for post-operative patients with endometrial carcinoma (RTOG 0418). *Int J Radiat Oncol Biol Phys* 2008;72:S16.
17. Mundt AJ, Mell LK, Roeske JC. Preliminary analysis of chronic gastrointestinal toxicity in gynecology patients treated with intensity-modulated whole pelvic radiation therapy. *Int J Radiat Oncol Biol Phys* 2003;56:1354-1360.
18. Chen MF, Tseng CJ, Tseng CC, Kuo YC, Yu CY, Chen WC. Clinical outcome in posthysterectomy cervical cancer patients treated with